Eur. Phys. J. Plus (2025) 140:30
https://doi.org/10.1140/epjp/s13360-025-05976-z

THE EUROPEAN PHYSICAL JOURNAL PLUS

Review

Observing pulsars with $f(R)$ gravity and using van der Waals equation of state in model

S. A. Mardan[1,a], **A. Khalid**[1,b], **Rubab Manzoor**[1,c], **Muhammad Bilal Riaz**[2,3,d]

[1] Department of Mathematics, University of Management and Technology, Lahore, Pakistan
[2] IT4Innovations, VSB - Technical University of Ostrava, Ostrava, Czech Republic
[3] Department of Computer Science and Mathematics, Lebanese American University, Byblos, Lebanon

Received: 29 September 2024 / Accepted: 2 January 2025

Abstract This research focuses on the evolution of the universe and observes pulsars using modified gravitational theory. We computed the Einstein field equations for an anisotropic spherical structure with $f(R)$ gravity. Furthermore, our density–pressure relationship is defined using the well-known van der Waals equation of state (VdW EoS). Graphs are used to investigate the behavior of physical parameters, and energy conditions are used to demonstrate the physical continuity of dense stars. Plotting the adiabatic index shows the model's stability. The resulting figures of physical parameters confirm the model's practical and conceptual feasibility. Under the effect of $f(R)$ gravity, our work demonstrates regularity, viability and stability, supporting the presence of heavy pulsars such as $PSR\ J0348+0432$, $PSR\ J0740+6620$ and $PSR\ J0030+0451$.

1 Introduction

In September 1967, while observing radio sources in the sky with telescopes, scientists noticed a strange radio signal that had never been observed before. That signal produced strong, fast, acute and amazingly constant radiation pulses. After further investigation, scientists dubbed them "pulsating radio sources" after initially interpreting them as messages from an advanced civilization. Additionally, they are now frequently referred to as pulsars. The pulsar signal was reported by Hewish et al. [1], who also provided information on the signal's rang, frequency, speed and other crucial parameters.

Stairs [2] provided methods for determining pulsar timing models and features, enabling tests of general relativity (GR) with both single and binary pulsars. According to Manchester [3], neutron stars formed during supernova explosions rotate clockwise due to celestial causes. Pulsars are celestial sources that provide valuable insights about neutron stars. Turolla and Nobili [4] evaluated pulse profiles from the thermally emitting outer surface of a neutron star. In 1974, physicists discovered binary pulsars, which opened up new avenues for studying relativistic gravity. Damour [5] presented the first binary pulsars that provided realistic test results for the strong-field regime in GR. Burnell [6] re-explained the detection procedure of pulsars and raised the subject of how they emit and how their loss of energy affects their spinning speed. Dong-Hoon and Sascha [7] developed a magnetic dipole model for pulsars to investigate electromagnetic radiation in GR. Neil [8] found evidence for neutron stars in the presence of pulsars. He characterized pulsars as rapidly revolving neutron stars that emit uniform pulses of electromagnetic radiation.

Fluid types in dense objects are differentiated based on pressure, making it an important topic in GR research history. Isotropic fluids require exactly the same radial and transverse pressures, but anisotropic fluids have varying pressures. Herrera et al. [9] presented analytical solutions for the Einstein field equations with isotropic and anisotropic matter distributions in spherically symmetric models. According to Hernandez and Nunez [10], non-local EoS can provide appropriate static anisotropic spherically oriented matter topologies when radial and tangential pressure fade. Herrera et al. [11] solved the Einstein field equations, verified matching requirements for anisotropic fluid distribution and integrated expansion-free relations. Maurya et al. [12] developed an anisotropic analog with metric potentials. Anisotropic fluid spheres are regarded as messier things. Due to their interior makeup, they may resemble neutron stars or other compact objects. Boonserm et al. [13] proposed that neutron stars can be modeled as anisotropic solid spheres, similar to spherically symmetric planets, or as a solid crust. Bhatti and Yousaf [14] modified Ellis equations and

muhammad.bilal.riaz@vsb.cz, bilalsehole@gmail.com.

[a] e-mail: syedalimardanazmi@yahoo.com (corresponding author)
[b] e-mails: ayeshakhalid4238@gmail.com; S2019109012@umt.edu.pk
[c] e-mail: rubab.manzoor@umt.edu.pk
[d] e-mails: muhammad.bilal.riaz@vsb.cz; bilalsehole@gmail.com

Published online: 14 January 2025

conservation relations for dynamical particles using the $f(R)$ model and anisotropic matter distribution. Maurya et al. [15] proved generic conclusions for anisotropic dense stars, including physical features, model stability and mass-radius relation. Sahoo et al. [16] proposed cosmological models using changeable retarded parameters in $f(R, T)$ gravity for the homogeneous anisotropic Bianchi type-I universe.

Einstein's gravitational theory has evolved as a powerful tool for understanding the geometrical features of spacetime. Currently, it is reasonable to believe that the cosmos is expanding rapidly. These findings highlighted the most significant concerns in GR. To understand this occurrence in GR, it is assumed that the acceleration is caused by an unknown dark energy or that our universe requires a modification to the gravity theory. Recent advancements in modified gravity theories, sometimes known as $f(R)$ theories, have replaced dark energy. Nojiri and Odintsov [17] presented many gravitational models, including $f(R)$, f(G) and $f(R, G)$, with Gauss-Bonnet-dilaton coupling. Nojiri and Odintsov [18] stated that $f(R)$ gravity can explain radiation epoch, cosmic acceleration and inflation. Capozziello and Laurentis [19] analyzed the conceptual characteristics of $f(R)$ theories, their function in equating dynamical and conformal theories and the starting value problem. Cruz-Dombriz and Saez-Gomez [20] analyzed modified gravity theories, developed a $f(R)$ model and compared black-hole solutions to GR results. Bamba et al. [21] studied dark energy cosmologies in $f(R)$, emphasizing the importance of finite-time future singularities. Koyama [22] developed $f(R)$ models to investigate dark energy and conduct cosmological testing. Yousaf et al. [23] investigated the impact of $f(R)$ gravity on anisotropic compact stars, expressing R in terms of Ricci scalar. Yousaf et al. [24] proposed the Lemaitre–Tolman–Bondi dynamical model for dense stars with $f(R)$ gravity. Nashed and Capozziello [25] derived a novel interior result for compact objects under $f(R)$ gravity using a differential equation to limit the Ricci curvature scalar, demonstrating that EoS cannot be nonlinear. [26] studies compact stars under $f(R)$ gravity. They observe the pulsar $SAX\ J1748.9-2021$ to study stellar structure equations and the impact of anisotropic fluid on neutron stars.

Van der Waals originally introduced the VdW EoS in 1873. Historically, VdW EoS focused on the chemical sector, connecting gaseous and liquid states of matter. Later, researchers used VdW EoS to visualize the relationship between two parameters. Malaver [27] presents a well-behaved model with VdW EoS for dense objects with anisotropic matter distribution and physical analysis. Kontogeorgis et al. [28] found that VdW EoS aligns with the states principle, predicts phase diagrams and demonstrates free-volume and energy impacts of models. Kong et al. [29] applied thermodynamic techniques to the Friedmann–Robertson–Walker universe and analyzed phase transitions in VdW. Errehymy et al. [30] used an Einstein field equation model and VdW EoS to study heavy pulsars emitted by neutron stars. Ditta et al. [31] utilized the modified VdW EoS to establish the metric function and develop the $f(Q)$ gravity model.

The adiabatic index is a fundamental sufficient condition for the stability or instability criterion. The relation encompasses all essential properties of the EoS. The stability of dense objects depends on the correlation between the EoS of the fluid interior and the power of relativistic field. The adiabatic index formula connects the relativistic composition of spheres to the EoS of dense stars' inner fluids. The adiabatic index is necessary for testing the stability of stellar models. Chandrasekhar [32] used the adiabatic index to assess hydrostatic equilibrium and dynamic instability. Herrera et al. [33] discovered that the pressure–density relationship does not apply to all areas of a material, resulting in varying levels of stability. Cooperstein [34] tested the stability of his neutron star model using an uncommon Galilean adiabatic index, where ρ represents baryon density. Chan et al. [35] explored the role of anisotropy in dynamical instability using the adiabatic index. Moustakidis [36] proposed that the adiabatic index can provide insights into conditions such as maximum central pressure, density and mass by examining their relationship.

Energy conditions are commonly used in GR to get broad effects in diverse physical settings. Proposing $f(R)$ theories presents a challenge in proving their theoretical validity. Energy conditions are imposed. These conditions create attractive gravity, which maintains positive energy density for $f(R)$. According to Bergliaffa [37], the presence of dark energy in the cosmos violates the strong energy requirement, prompting the development of $f(R)$ hypotheses to explain the expansion. Santos et al. [38] justified the boundaries on a generic $f(R)$ theory utilizing energy requirements in the framework of metric alternative approaches. Wang and Liao [39] obtained answers for energy circumstances and limited $f(R, Lm)$ gravity from conceptual considerations. Energy conditions for Dolgov–Kawasaki and mimetic-$f(R)$ gravity were reviewed by Shiravand et al. [40]. Bamba et al. [41] solved energy requirements and assumed Friedmann–Lemaitre–Robertson–Walker metric for their models of modified $f(G)$.

The paper is organized as follows: In Section II, we shall establish Einstein field equations for static spherically symmetric astrophysical objects for anisotropic sources subjected to modified $f(R)$ gravity. In Section III, we combine VdW EoS and a gravitational potential connection to provide a more realistic approach to Einstein field equations. Section IV describes the matching conditions for inner and outside spacetime. Section V focuses on analyzing physical parameters under various settings. Section VI evaluates the mass, compactness and gravitational redshift of objects. The M-R stability requirement is discussed in Section VII. The following section, VIII, contains the adiabatic index equation. In the final section, we reported our findings, followed by the computed results and a list of references cited.

2 Modified $f(R)$ theory of gravity

This section is dedicated to the introduction of $f(R)$ gravity, which is mainly based on modified Einstein–Hilbert action as a function of Ricci scalar R and is given by

$$S_{f(R)} = \frac{1}{2\kappa^2}\int d^4x\sqrt{-g}f(R) + S_M, \tag{1}$$

here, g stands for the determinant of the tensor, and S_M is matter field action. By using a variation in Eq. (1) w.r.t g_{ij}, the $f(R)$ field equation is presented as

$$R_{ij}f_R - \frac{1}{2}f_R g_{ij} + (g_{ij}\Box - \nabla_i\nabla_j)f_R = \kappa^2 T_{ij}, \tag{2}$$

where the gravitational coupling constant is $\kappa^2 = \frac{8\pi G}{c^4}$. In geometrized units, the gravitational constant G and speed of light c are taken as 1. T_{ij} is the usual energy-momentum tensor. Meanwhile, there ∇_i is covariant derivative, which defines $\Box \equiv \nabla^j\nabla_j$ and $f_R \equiv df/dR$. Equation (2) can be written as

$$G_{ij} = \frac{\kappa^2}{f_r}(T_{ij}^{(D)} + T_{ij}) \equiv T_{ij}^{(eff)}, \tag{3}$$

where the G_{ij} and $T_{ij}^{(D)}$ indicate the Einstein tensor and effective energy-momentum tensor. Expressed as

$$T_{ij}^{(D)} = \frac{1}{\kappa^2}\left\{\nabla_i\nabla_j f_R - \Box f_R g_{ij} + (f - Rf_R)\frac{g_{ij}}{2}\right\}. \tag{4}$$

The anisotropic spherically symmetric line element is taken as

$$\mathrm{d}s^2 = e^{\nu(r)}\mathrm{d}t^2 - e^{\lambda(r)}\mathrm{d}r^2 - r^2(\mathrm{d}\theta^2 + \sin^2\theta d\phi^2), \tag{5}$$

in Schwarzschild coordinates $x^a = (t, r, \theta, \varphi)$. Where gravitational potential is ν and λ. Now, the equation of energy-momentum tensor is

$$T_{ij} = (\rho + p_t)u_i u_j - p_t g_{ij} + (p_r - p_t)S_i S_j, \tag{6}$$

where the four vectors u_i and S_i obey the relations $u^i S_i = 0$, $u_i u^i = 1$ and $S_i S^i = -1$. Also, the energy-momentum tensor shows the following relationship

$$T_{ij} = 0 \quad if \quad i \neq j. \tag{7}$$

the following results are calculated by $f(R)$ field Eq. (3), metric Eq. (5) and fluid (6).

$$\rho = \frac{e^{-\lambda}}{2r^2}(-2\lambda' r f_R + 2f_R - 2f_R e^{\lambda} - 2r^2 f_R'' + \lambda' r^2 f_R' - 4rf_R' + r^2 e^{\lambda} R f_R - r^2 f e^{\lambda}), \tag{8}$$

$$p_r = \frac{e^{-\lambda}}{2r^2}(2e^{\lambda} f_R - 2f_R - r^2 f_R e^{\lambda} R + r^2 e^{\lambda} f + 2f_R r\nu' + 4rf_R' + \nu' r^2 f_R'), \tag{9}$$

$$\begin{aligned} p_t = \frac{e^{-\lambda}}{4r}(&-2f_R r\nu'' - (\nu')^2 r f_R - \nu'\lambda' r f_R + 2f_R\lambda' - 2f_R\nu' + 4f_R' \\ &+ 2\nu' f_R' r + 4rf_R'' - 2\lambda' r f_R'' + 2e^{\lambda} rf - 2e^{\lambda} r R f_R). \end{aligned} \tag{10}$$

To achieve more realistic solutions for the anisotropic stellar model, specific transformations for metric [40] variables are applied.

$$x = r^2, \quad Z(x) = e^{-\lambda}, \quad y = e^{\nu}. \tag{11}$$

By making use of Eq. (11), we shape following equations for $f(R)$.

$$\rho = \left[-f_R'' Z - \left(\frac{Z'}{2} - \frac{2Z'}{\sqrt{x}}\right)f_R' + \left(\frac{2Z}{\sqrt{x}} - \frac{1}{2} - \frac{1}{x} + \frac{R}{2}\right)f_R\right], \tag{12}$$

$$p_r = \left[\left(\frac{Zf_R}{\sqrt{x}} + \frac{Zf_R'}{2}\right)\frac{y'}{y} + \frac{2Zf_R'}{\sqrt{x}} + \left(\frac{1}{x} - \frac{Z}{x} - \frac{R}{2} + \frac{1}{2}\right)f_R\right], \tag{13}$$

$$\begin{aligned} p_t = \Bigg[&-\frac{Zf_R}{2}\left(\frac{y''}{y}\right) + \frac{Zf_R}{4}\left(\frac{y'}{y}\right)^2 + \left(\frac{Zf_R'}{2} - \frac{Z'f_R}{4} - \frac{Zf_R}{2\sqrt{x}}\right)\frac{y'}{y} \\ &+ \left(Z + \frac{Z'}{2}\right)f_R'' + \frac{Zf_R'}{\sqrt{x}} + \left(\frac{1}{2} - \frac{Z'}{2\sqrt{x}} - \frac{R}{2}\right)f_R\Bigg]. \end{aligned} \tag{14}$$

$$p_t = p_r + \Delta, \tag{15}$$

$$\Delta = \Bigg[-\frac{Zf_R}{2}\left(\frac{y''}{y}\right) + \frac{Zf_R}{4}\left(\frac{y'}{y}\right)^2 + \left(-\frac{Z'}{4} - \frac{3Zf_R}{2\sqrt{x}}\right)\frac{y'}{y} + \left(Z + \frac{Z'}{2}\right)f_R'' - \frac{Z}{\sqrt{x}}f_R' + \left(\frac{Z}{x} - \frac{Z'}{2\sqrt{x}} - \frac{1}{x}\right)f_R\Bigg]. \tag{16}$$

as fluid distribution satisfy the barotropic EoS $p_r = p_r(\rho)$. We considered modified VdW EoS to understand inner matter distribution of dense objects.

$$p_r = \alpha\rho^2 + \frac{\beta\rho}{1+\gamma\rho}, \tag{17}$$

For better involvement of VdW EoS, the discussion of constants like α, β and γ is given with conditions. The dark energy EoS can be restored if α, γ approaches 0 and $\beta = \frac{p_r}{\rho}$ has smaller value than $-1/3$. The modified VdW EoS shows that VdW fluid is the fluid which deals with dark energy. From Eq. (15) below equation is formed

$$y = exp^{\int\left[\frac{\sqrt{x}}{(2f_R+\sqrt{x}f_R')Z}(\alpha\rho^2+\frac{\beta\rho}{1+\gamma\rho}-\frac{2Zf_R'}{\sqrt{x}}+(a-bx-\frac{R}{2}+\frac{1}{2})f_R)\right]dx}, \tag{18}$$

now, by substituting Eq. (18) in Eq. (5), next relation is stated as

$$ds^2 = exp^{\int\left[\frac{\sqrt{x}}{(2f_R+\sqrt{x}f_R')Z}(\alpha\rho^2+\frac{\beta\rho}{1+\gamma\rho}-\frac{2Zf_R'}{\sqrt{x}}+(a-bx-\frac{R}{2}+\frac{1}{2})f_R)\right]dx}dt^2 - Z^{-1}dr^2 - r^2(d\theta^2 + sin^2\theta d\phi^2). \tag{19}$$

This is the anisotropic spherically symmetric relation involving VdW EoS. Defined by gravitational potential $Z(x)$.

3 Realistic results for $f(R)$ gravity

For more realistic modeling of the set of Einstein field, Eqs. (12-16) are further simplified by the following relation of gravitational potential $Z(x)$.

$$Z = 1 - ax + bx^2, \tag{20}$$

here, a and b are constants.

$$e^{-\lambda} = 1 - ax + bx^2, \tag{21}$$

simplified $f(R)$ field equations are

$$\rho = \Bigg[-(1-ax+bx^2)f_R'' - \frac{2}{\sqrt{x}}\left(-bx^2 + \left(-\frac{a}{4} + \frac{bx}{2}\right)\sqrt{x} + ax - 1\right)f_R' + (2bx^3 + (R-1)x^{\frac{3}{2}} - 2\sqrt{x} + 4bx^2 - 2ax^2 + (-2a+2)x)\frac{f_R}{2x^{\frac{3}{2}}}\Bigg], \tag{22}$$

$$p_r = \alpha\rho^2 + \frac{\beta\rho}{1+\gamma\rho}, \tag{23}$$

$$p_t = p_r + \Delta, \tag{24}$$

$$\Delta = \Bigg[\left(\frac{2-2ax+2bx^2-a+2bx}{2}\right)f_R'' - \left(\frac{1-ax+bx^2}{\sqrt{x}}\right)f_R' + \left(-b + \frac{(-a+2bx)^2}{4(1-ax+bx^2)} + \frac{3(-a+2bx)}{2\sqrt{x}} - a + bx + \frac{a}{2\sqrt{x}-b\sqrt{x}}\right)f_R - \left(\frac{(-a+2bx)^2}{4(1-ax+bx^2)}\right)\Bigg]. \tag{25}$$

The Ricci scalar is derived as

$$R = \left(2a - 2b - 2bx + \frac{4(a-bx)}{\sqrt{x}} - \frac{(a-2bx)^2}{(1-ax+bx^2)}\right), \tag{26}$$

We presented a model of $f(R)$ with a power law as a function of the Ricci scalar [23]

$$f(R) = R + \alpha R^2. \tag{27}$$

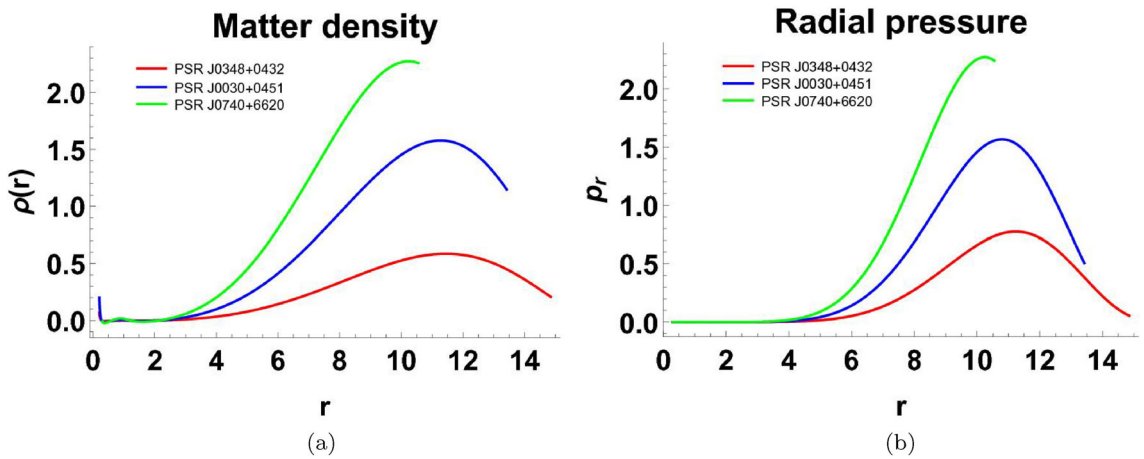

(a) (b)

Fig. 1 Variation of density and radial pressure w.r.t radial coordinate r. Behavior of 3 heavy pulsars

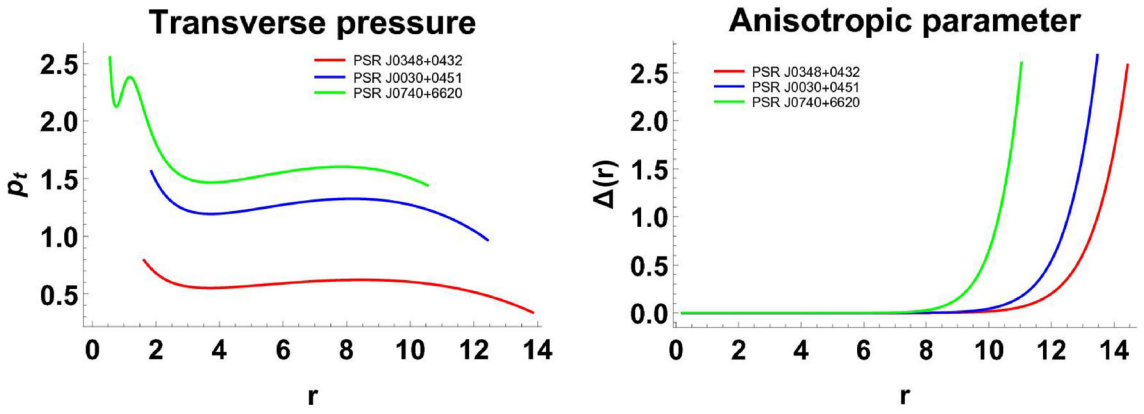

(a) (b)

Fig. 2 Variation of transverse pressure and anisotropic parameter w.r.t radial coordinate r. Behavior of 3 heavy pulsars

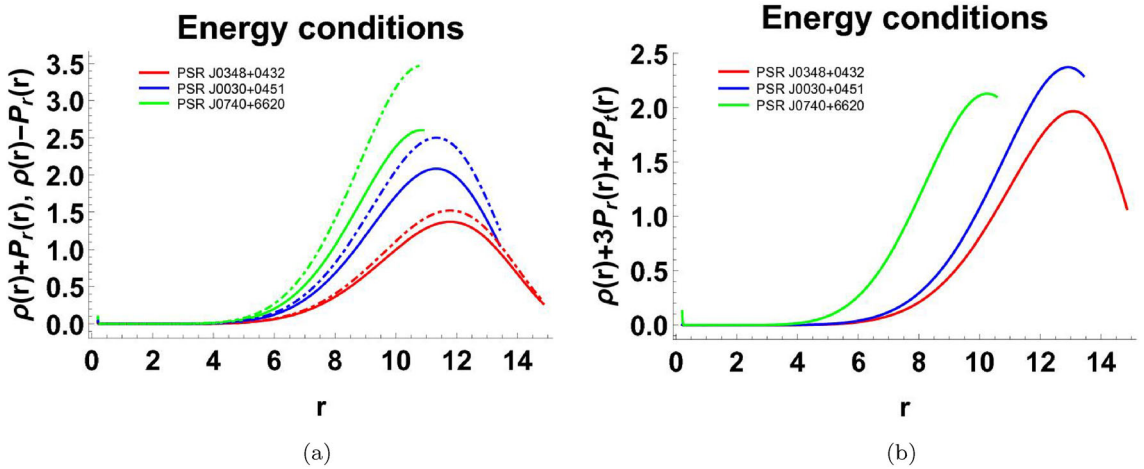

(a) (b)

Fig. 3 Variation of energy conditions w.r.t radial coordinate r. Behavior of 3 heavy pulsars

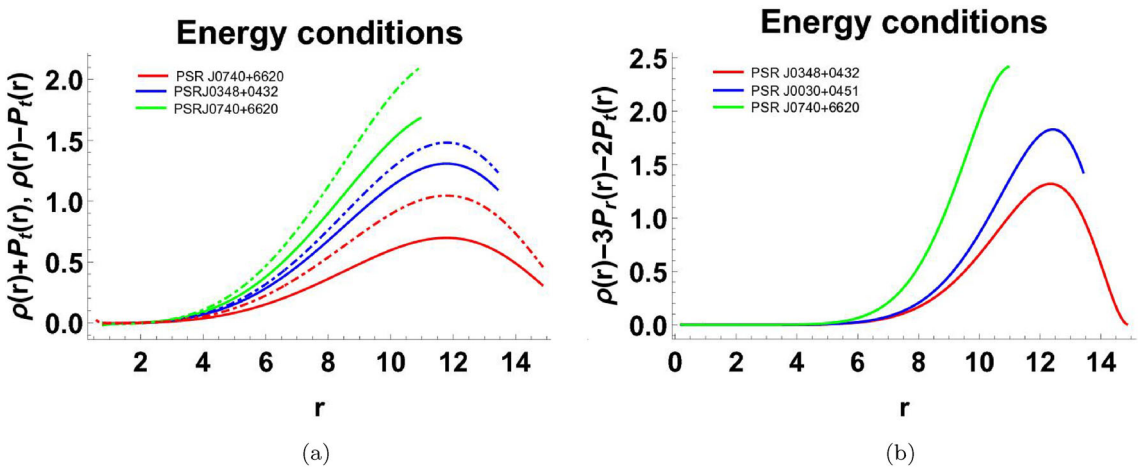

Fig. 4 Variation of energy conditions w.r.t radial coordinate r. Behavior of 3 heavy pulsars

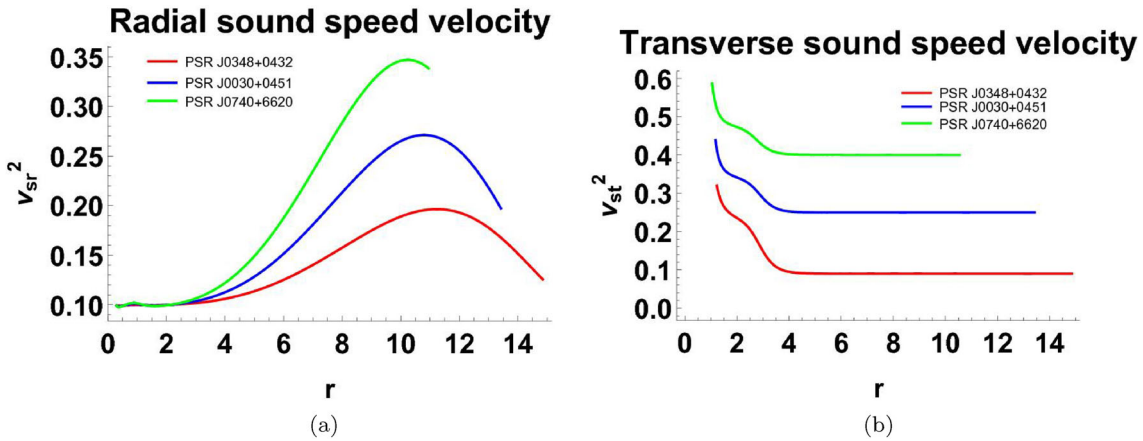

Fig. 5 Variation of radial and transverse velocity w.r.t radial coordinate r. Behavior of 3 heavy pulsars

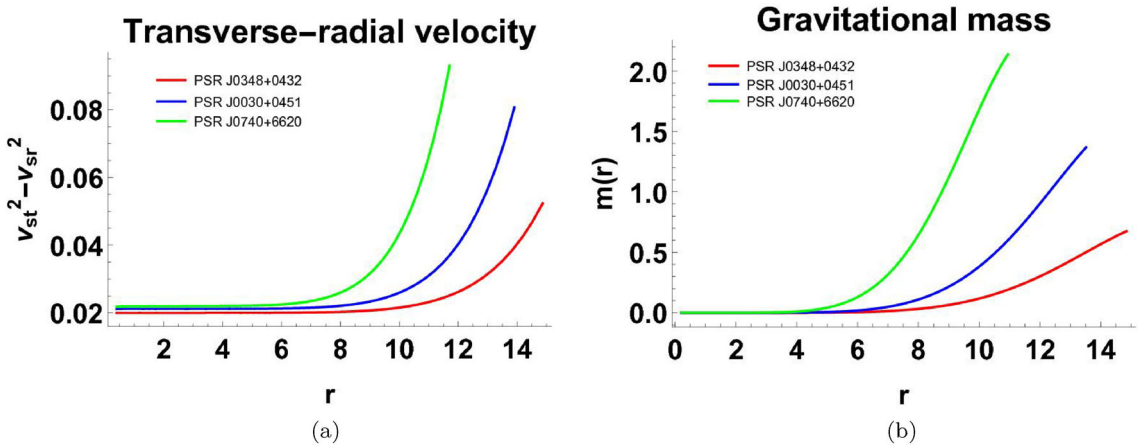

Fig. 6 Variation of gravitational mass and $V_{sr}^2 - V_{st}^2$ w.r.t radial coordinate r. Behavior of 3 heavy pulsars

4 Matching conditions for $f(R)$ solution

This section shows smooth collaboration of inner spacetime to the outer vacuum of stellar surface defining $r = R_s$, where R_s is greater than $2M$. The line element for the $f(R)$ stellar configuration is

$$ds_+^2 = -(1 - \frac{2M}{r})dt^2 + -(1 - \frac{2M}{r})^{-1}dr^2 + r^2 d\Omega_2^2. \quad (28)$$

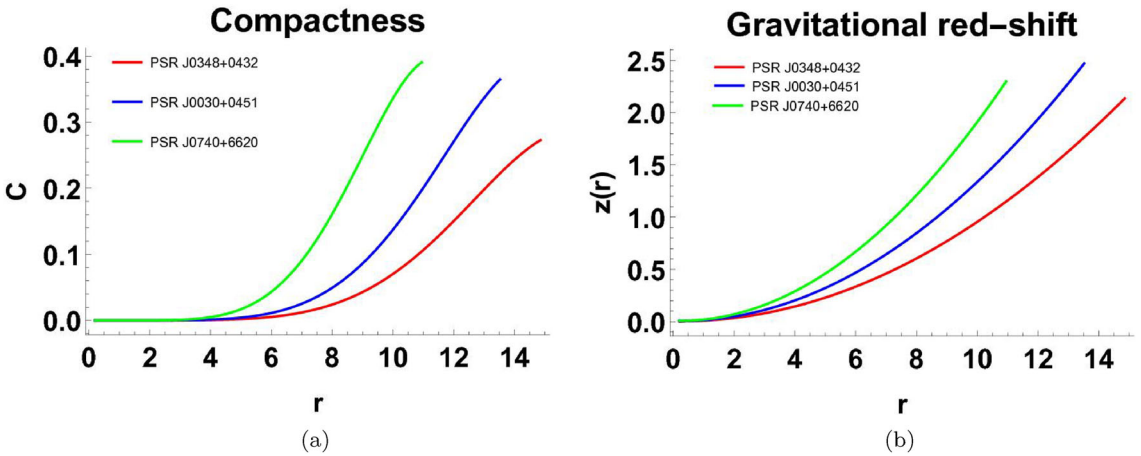

(a) (b)

Fig. 7 Variation of compactness and redshift parameter w.r.t radial coordinate r. Behavior of 3 heavy pulsars

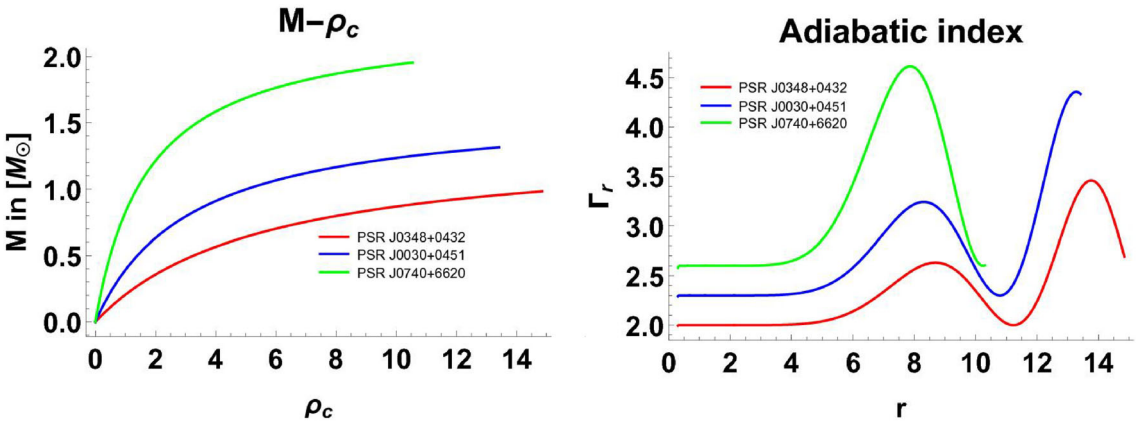

(a) (b)

Fig. 8 Variation of $M - R$ and $M - \rho_c$ w.r.t radial coordinate r. Behavior of 3 heavy pulsars

Here $d\Omega_2^2 = d\theta^2 + sin^2\theta d\phi^2$. M is the total mass. To ensure continuity at junction of inner and outer spacetime, the given below conditions must be satisfied for hyper-surface $\sum$.

$$([ds_-^2]_\Sigma = [ds_+^2]_\Sigma), \quad ([K_{ij-}]_\Sigma = [K_{ij+}]_\Sigma), \tag{29}$$

$$(e^{\nu^-}|_{r=R_s} = e^{\nu^+}|_{r=R_s}) \quad \text{and} \quad (e^{\lambda^-}|_{r=R_s} = e^{\lambda^+}|_{r=R_s}), \tag{30}$$

added,

$$\left(\frac{\partial e^{\nu^-}}{\partial r}\right)_{|r=R_s} = \left(\frac{\partial e^{\nu^+}}{\partial r}\right)_{|r=R_s}. \tag{31}$$

Here +, −, K_{ij} define inner spacetime, outer spacetime and curvature. By continuity condition $[ds^2]_\Sigma = 0$ we get $[F]_\Sigma \equiv F^+(R_s) - F^-(R_s) \equiv F(r \longrightarrow R_s^+) - F(r \longrightarrow R_s^-)$.

$$(g_{rr}^+(R_s) = g_{rr}^-(R_s)) \quad \text{and} \quad (g_{tt}^+(R_s) = g_{tt}^-(R_s)). \tag{32}$$

Accordingly, the case $r = r_\Sigma$ leads to the lower result

$$p_r(R) = 0. \tag{33}$$

So, $\sum_-$ is inner and $\sum_+$ is outer sectors. The hyper-surface line element is

$$ds^2 = d\tau^2 - R_s^2 d\vartheta^2 + R_s^2 \sin^2\vartheta d\phi^2. \tag{34}$$

Table 1 Constant values for pulsar $PSRJ0348+0432$

Parameters	b	a	α	β	γ	$R[km]$	$M[M_{\odot}]$
ρ	0.2	250	− 9.0002	0.001	1	$14.85^{+0.11}_{-0.11}$	$2.01^{+0.04}_{-0.04}$
p_r	0.2	240	9.0002	0.0001	1	$14.85^{+0.11}_{-0.11}$	$2.01^{+0.04}_{-0.04}$
p_t	190.2	− 240	9.0002	0.0001	1	$14.85^{+0.11}_{-0.11}$	$2.01^{+0.04}_{-0.04}$
m	0.2	40	− 9.0002	0.01	1	$14.85^{+0.11}_{-0.11}$	$2.01^{+0.04}_{-0.04}$
z	− 0.002	0.005	− 1.0002	0.01	1	$14.85^{+0.11}_{-0.11}$	$2.01^{+0.04}_{-0.04}$
C	0.02	400	− 9.0002	0.01	1	$14.85^{+0.11}_{-0.11}$	$2.01^{+0.04}_{-0.04}$
Δ	190.2	− 240	− 0.000002	0.0001	1	$14.85^{+0.11}_{-0.11}$	$2.01^{+0.04}_{-0.04}$
v_{sr}	0.2	240	9.0002	0.0001	1	$14.85^{+0.11}_{-0.11}$	$2.01^{+0.04}_{-0.04}$
v_{st}	90.02	− 250	240.02	0.0001	1	$14.85^{+0.11}_{-0.11}$	$2.01^{+0.04}_{-0.04}$
Γ	0.2	240	9.0002	0.0001	1	$14.85^{+0.11}_{-0.11}$	$2.01^{+0.04}_{-0.04}$

The time element is τ. And extrinsic curvature [28] is written as

$$K_{ij}^{\pm} = -\eta_k^{\pm}\left(\frac{\partial^2 y_{\pm}^k}{\partial n^i n^j}\right) - \eta_k^{\pm}\Gamma_{\mu l}^k\left(\frac{\partial y_{\pm}^{\mu}}{\partial n^i}\frac{\partial y_{\pm}^l}{\partial n^j}\right), \tag{35}$$

here, n^i, and $\eta_k^{\pm}$ are coordinates and 4-speed of boundary $\sum$, respectively. Where $y_{\pm}^{\nu}$ and $\tau^{\pm}$ are coordinates of $\eta_k^{\pm}$.

$$\eta_k^{\pm} = \pm\frac{df}{dy^k}\left|g^{\mu l}\frac{df}{dy^{\mu}}\frac{df}{dy^l}\right|^{-1/2} \quad where \quad (\eta_k\eta^k = 1). \tag{36}$$

The unit normal vectors of interior and exterior sector are

$$\eta_k^- = (0, -e^{\lambda}, 0, 0) \quad and \quad \eta_k^+ = \left[0, \left(1 - \frac{2M}{r}\right)^{-1}, 0, 0\right]. \tag{37}$$

From the coordination of Eq. (5), (34) and (28), we obtain

$$\left[\frac{dt}{d\tau}\right]_{\Sigma} = \left[\left(1 - \frac{2M}{r}\right)^{-1}\right]_{\Sigma} = [e^{\lambda}]_{\Sigma}, \tag{38}$$

here $[r]_{\Sigma} = R_s$. The nonzero factors of K_{ij} are

$K_{00}^- = \left[\frac{\nu'}{2}e^{\nu}\right]_{\Sigma}$, $K_{11}^- = (r)$, $K_{22}^- = (r\sin^2)$,

$K_{00}^+ = \left[\frac{M}{r^2}\right]_{\Sigma}$, $K_{11}^+ = (r)$, $K_{22}^+ = (r\sin^2\theta)$

.

Where$[K_{11}^-]_{\Sigma} = [K_{11}^+]_{\Sigma}$

$$e^{-\lambda} = \left(1 - \frac{2M}{R}\right). \tag{39}$$

By solving $[K_{00}^-]_{\Sigma} = [K_{00}^+]_{\Sigma}$, we get,

$$\nu'(R_s) = \left(\frac{2M}{R_s(R_s - 2M)}\right). \tag{40}$$

From Eq. (38-40), we found

$$e^{\lambda(R_s)} = 1 - aR_s + bR_s^2 = \left[\frac{1 - 2M}{R_s}\right]^{-1}, \tag{41}$$

$$e^{\nu(R_s)} = y(R_s) = \left[\frac{1 - 2M}{R_s}\right]. \tag{42}$$

[43] and [44] discussed their models with extrinsic curvature and work on Einstein constraints.

Table 2 Constant values for pulsar $PSRJ0030+0451$

Parameters	b	a	α	β	γ	$R[km]$	$M[M_{\odot}]$
ρ	0.3	248	– 10.0002	0.01	1	$13.42^{+0.24}_{-0.22}$	$2.14^{+0.10}_{-0.09}$
p_r	0.32	230	11.0002	0.0002	1	$13.42^{+0.24}_{-0.22}$	$2.14^{+0.10}_{-0.09}$
p_t	180.32	– 230	11.0002	0.0002	1	$13.42^{+0.24}_{-0.22}$	$2.14^{+0.10}_{-0.09}$
m	0.3	350	– 10.0002	0.01	1	$13.42^{+0.24}_{-0.22}$	$2.14^{+0.10}_{-0.09}$
z	– 0.003	0.0015	– 2.0002	0.01	1	$13.42^{+0.24}_{-0.22}$	$2.14^{+0.10}_{-0.09}$
C	0.3	350	– 10.0002	0.1	1	$13.42^{+0.24}_{-0.22}$	$2.14^{+0.10}_{-0.09}$
Δ	90.002	– 10.0015	0.50	0.01711	1	$13.42^{+0.24}_{-0.22}$	$2.14^{+0.10}_{-0.09}$
v_{sr}	0.32	230	11.0002	0.0002	1	$13.42^{+0.24}_{-0.22}$	$2.14^{+0.10}_{-0.09}$
v_{st}	100.01	– 240	201.02	0.0002	1	$13.42^{+0.24}_{-0.22}$	$2.14^{+0.10}_{-0.09}$
Γ	0.32	230	11.0002	0.0002	1	$13.42^{+0.24}_{-0.22}$	$2.14^{+0.10}_{-0.09}$

Table 3 Constant values for pulsar $PSRJ0740+6620$

Parameters	b	a	α	β	γ	$R[km]$	$M[M_{\odot}]$
ρ	0.37	245	– 9.52	0.01	1	$10.55^{+0.41}_{-0.40}$	$1.14^{+0.15}_{-0.14}$
p_r	0.37	210	10.922	0.0003	1	$10.55^{+0.41}_{-0.40}$	$1.14^{+0.15}_{-0.14}$
p_t	170.37	– 210	10.922	0.0003	1	$10.55^{+0.41}_{-0.40}$	$1.14^{+0.15}_{-0.14}$
m	0.37	210	– 9.52	0.01	1	$10.55^{+0.41}_{-0.40}$	$1.14^{+0.15}_{-0.14}$
z	0.0037	0.002	– 2.52	0.01	1	$10.55^{+0.41}_{-0.40}$	$1.14^{+0.15}_{-0.14}$
C	0.37	210	– 9.52	0.01	1	$10.55^{+0.41}_{-0.40}$	$1.14^{+0.15}_{-0.14}$
Δ	170.37	– 210	– 0.00003	0.0003	1	$10.55^{+0.41}_{-0.40}$	$1.14^{+0.15}_{-0.14}$
v_{sr}	0.37	210	12.922	0.0003	1	$10.55^{+0.41}_{-0.40}$	$1.14^{+0.15}_{-0.14}$
v_{st}	80.037	– 210	260.922	0.0003	1	$10.55^{+0.41}_{-0.40}$	$1.14^{+0.15}_{-0.14}$
Γ	0.37	210	10.922	0.0003	1	$10.55^{+0.41}_{-0.40}$	$1.14^{+0.15}_{-0.14}$

5 Physical analysis of $f(R)$ model

The physical conditions for well-behaved $f(R)$ model are listed in current section. The physical acceptability of pulsars $PSRJ0348+0432$, $PSRJ0030+0451$ and $PSRJ0740+6620$ are presented by plotting graphs. Here different physical conditions of dense object formation are discussed which explains that the model is physically applicable.

- **Necessary rules for matter density and pressure:** The matter density (ρ) and pressures (p_r, p_t) of $f(R)$ gravity model show the continuity and positivity at surface of star. According to Fig. 1 and 2a, the matter density and pressure monotonically reduce smoothly in the direction of surface line of the stellar configurations, increase at stellar center and p_r disappear at boundary where $r = R_s$.

$$\rho_c = \rho(r=0) = 32\alpha b^4 + 4\alpha a^2 b^2 + 24\alpha a b^3 + 4\alpha a^2 b + 8\alpha a b^2 + a^2 b + 2ab^2 > 0. \tag{43}$$

The central pressure of $f(R)$ gravity model is

$$\begin{aligned} p_c = p(r=0) = {} & \alpha(32\alpha b^4 + 4\alpha a^2 b^2 + 24\alpha a b^3 + 4\alpha a^2 b + 8\alpha a b^2 + a^2 b + 2ab^2)^2 \\ & + \frac{\beta(32\alpha b^4 + 4\alpha a^2 b^2 + 24\alpha a b^3 + 4\alpha a^2 b + 8\alpha a b^2 + a^2 b + 2ab^2)}{1+\gamma(32\alpha b^4 + 4\alpha a^2 b^2 + 24\alpha a b^3 + 4\alpha a^2 b + 8\alpha a b^2 + a^2 b + 2ab^2)} > 0. \end{aligned} \tag{44}$$

Figure 2b shows that the anisotropy profile increases monotonically from the star's core to its boundary. It has a limited and regular interior and is repulsive in nature.

- **The extrinsic curvature continuity:** The extrinsic curvature of a star is continuous and corresponds to a hyper-surface, resulting in the equation below.

$$(p_r)_{r=R_s} = 0 \tag{45}$$

- **Energy conditions:** To present physical feasibility of matter fields, the mathematical equations of stress–energy tensors should obey some constraints known as energy conditions (ECs). The energy conditions are important to study casual and geodesic

spacetime in GR. Yousaf [45] constructed many analytical models with dark coming through the cosmological constant and test the validity of ECs to ensure the physical acceptability of his work. Here are ECs defined by [23]. Null energy condition $\Leftrightarrow \quad \rho^{eff} + p_K^{eff} \geq 0, \forall k$ Weak energy conditions $\Leftrightarrow \quad \rho^{eff} \geq 0, \rho^{eff} + p_k^{eff} \geq 0, \forall k$ Strong energy condition $\Leftrightarrow \quad \rho^{eff} + 3p_r^{eff} + 2p_t^{eff} \geq 0, \rho^{eff} + p_k^{eff} \geq 0, \forall k$ Dominant energy conditions $\Leftrightarrow \quad \rho^{eff} \geq 0, \rho^{eff} \pm p_k^{eff} \geq 0, \forall k$ From Fig. 3 and 4 it is verified that all above ECs are well-behaved, results a non-exotic matter and positively acceptable in system.

- **Cracking of anisotropic star stability:** It is demanded that the speed of sound is smaller than c inside stellar object. The relations of speeds of sound are $v_{sr}^2 = (\frac{dp_r}{d\rho})$ and $v_{st}^2 = (\frac{dp_t}{d\rho})$. And satisfy the inequalities $(0 \leq v_{sr}^2 \leq 1)$ and $(0 \leq v_{st}^2 \leq 1)$. Figure 5 is the graphical evident that both speeds of sounds are less than 1. Figure 6a shows $(0 \leq v_{st}^2 - v_{sr}^2 \leq 1)$.

6 Mass m, compactness C and gravitational redshift z

The causal limit of mass for stars along modified $f(R)$ gravity is investigated by [46]. Astashenok et al. [47] reported that neutron objects cannot contain gravitational masses greater than $3M_{\odot}$. Also, in case of stars with mass observations is equal or above this limit, one requires modified extensions of GR, apart from $f(R)$ gravity. Plus, mass function is stated as

$$m = 4\pi \int_0^R \rho r^2 dr, \tag{46}$$

while the baryon mass function is given as

$$m = 4\pi \int_0^R r^2 e^{\lambda/2} \rho dr. \tag{47}$$

The mass-to-radius ratio C is the compactness factor and is defined by [26]

$$C = \left[\frac{2GM}{c^2 R}\right]. \tag{48}$$

For physical consistency $C << 0.5$ [25]. However, the redshift defined by compactness factor is stated as

$$z = \left[\left(\frac{1}{\sqrt{1-2u}}\right) - 1\right]. \tag{49}$$

Figs. 6b and 7 display that m, C and z are monotonically increasing functions w.r.t the coordinate r and non-negative inside the stellar system.

7 Stability conditions and M-R graph

Here is the conditions of stability criterion by [48].

$$\frac{\partial M}{\partial \rho_c} > 0 \quad \text{(For stable configuration)} \tag{50}$$

$$\frac{\partial M}{\partial \rho_c} < 0 \quad \text{(For unstable configuration)} \tag{51}$$

The total mass is computed from below equation

$$M(\rho_c) = \left(\frac{3R^3\rho_c}{18 + 4R^2\rho_c}\right) \tag{52}$$

Figure 8a records the variation of mass w.r.t central density, which concluded that increment in central density means more improvement in stability.

8 The adiabatic index

Adiabatic index is denoted by Γ and known as specific heat equation, used as stability test and defined by [42] and written as

$$\Gamma_r = \left(\frac{\rho + p_r}{p_r}\right)\frac{\partial p_r}{\partial \rho}. \tag{53}$$

Figure 8b fulfills the stability condition $\Gamma > \frac{4}{3}$ which shows the stability of our $f(R)$ gravity model.

9 Conclusions and results

This research focuses on analyzing physical properties of spherically symmetric dense systems using $f(R)$ theory. We employed transformation for metric functions with arbitrary constants to provide more realistic results. We used observational data on the $f(R)$ model for massive pulsars. We used observable and calculated data to plot physical variables such as matter density, pressures, anisotropic stresses along radial distance, compactness, redshift, mass, speed of sound and adiabatic index. Figure 1a shows that increasing radius leads to decreased density. Typically, behavior is observed in areas of tangential and radial pressure (Figs. 1b and 2a). Figure 2b shows an unusual pattern of growing anisotropy in the opposite direction of other functions.

As SEC and DEC are the fourth constraint reducing, the WEC measures the time-like plan for continuously positive density, while the NEC deduces that viewer traversing a null condition measures the local positive matter density (Figs. 3 and 4). The sound velocity decreases as one approaches the star object's boundary, but causality is not broken (Figs. 5 and 6a). It is evident from Figs. 6b and 7 that redshift and the compactness factor rise with increasing gravitational mass. More ρ_c leads to stronger stability, according to Fig. 8a. The stability of the model with a range exceeding $\frac{4}{3}$ is shown in Fig. 8b. Tables 1, 2 and 3 list the values of the constant for each of the three heavy pulsars.

Therefore, a practical substitute for Einstein gravity is modified $f(R)$ gravity. All physical and mathematical properties are admitted and shared by our $f(R)$ model, which also offers proof of the existence of genuine heavy pulsars.

Funding Open access publishing supported by the institutions participating in the CzechELib Transformative Agreement.

Data Availability My manuscript has no associated data.

References

1. A. Hewish, S.J. Bell, J.D.H. Pilkington, P.F. Scott, R.A. Collins, Observation of a rapidly pulsating radio source. Nature **217**, 709 (1968)
2. I.H. Stairs, Testing general relativity with pulsar timing. Living Rev. Relativ. **6**, 5 (2003)
3. R.N. Manchester, Observational properties of pulsars. Science **304**, 542 (2004)
4. R. Turolla, L. Nobili, Pulse profiles from thermally emitting neutron star. Astrophys. J. **768**, 147 (2013)
5. T. Damour, 1974: the discovery of the first binary pulsar. Class. Quantum Gravity **32**, 124009 (2015). arXiv:1411.3930 [gr-qc]
6. J.B. Burnell, The past, present and future of pulsars. Nat. Astron. **1**, 831 (2017)
7. K. Dong-Hoon , T. Sascha, General relativistic effects on pulsar radiation, (2021). arXiv:2109.13387 [astro-ph.HE]
8. L. Neil, S.M. Scott, K. Wette, What are neutron stars made of? Gravitational waves may reveal the answer. Int. J. Mod. Phys. D. **32**, 14 (2023). arXiv:2305.06606 [gr-qc]
9. L. Herrera, J. Jiménez, L. Leal, J. Ponce de León, M. Esculpi, V. Galina, Anisotropic fluids and conformal motions in general relativity. J. Math. Phys. **25**, 3274 (1984)
10. H. Hernandez, L.A. Nunez, Nonlocal equation of State in anisotropic static fluid spheres in general relativity. Can. J. Phys. **82**, 29 (2004). arXiv:gr-qc/0107025
11. L. Herrera, N.O. Santos, A. Wang, Shearing expansion-free spherical anisotropic fluid evolution. Phys. Rev. D. **78**, 084026 (2008)
12. S.K. Maurya, Y.K. Gupta, S. Ray, B. Dayanandan, Anisotropic models for compact stars. Eur. Phys. J. C **75**, 225 (2015). arXiv:1504.00209 [gr-qc]
13. P. Boonserm, T. Ngampitipan, M. Visser, Mimicking static anisotropic fluid spheres in general relativity. Int. J. Mod. Phys. **25**, 1650019 (2015). arXiv:1501.07044 [gr-qc]
14. M.Z. Bhatti, Z. Yousaf, Influence of electric charge and modified gravity on density irregularities. Eur. Phys. J. C **76**, 219 (2016). arXiv:1604.01395 [gr-qc]
15. S. K. Maurya, Y. K. Gupta, S. Ray, D. Deb, Generalized model for anisotropic compact stars, Eur. Phys. J. C. **76**, 1434, (2016). arXiv:1607.05582 [physics.gen-ph]
16. P.K. Sahoo, P. Sahoo, B.K. Bishi, Anisotropic cosmological models in $f(R, T)$ gravity with variable deceleration parameter. Int. J. Geom. Meth. Mod. Phys. **14**, 1750097 (2017). arXiv:1702.02469 [gr-qc]
17. S. Nojiri, S.D. Odintsov, Introduction to modified gravity and gravitational alternative for dark energy. Int. J. Geom. Meth. Mod. Phys. **4**, 115 (2007). arXiv:hep-th/0601213
18. S. Nojiri, S. D. Odintsov, Dark energy, inflation and dark matter from modified $F(R)$ gravity, (2008). arXiv:0807.0685 [hep-th]
19. S. Capozziello, M. De Laurentis, Extended theories of gravity. Phys. Rep. **509**, 167 (2011). arXiv:1108.6266 [gr-qc]
20. A. de la Cruz-Dombriz, D. Saez-Gomez, Black holes, cosmological solutions, future singularities, and their thermodynamical properties in modified gravity theories. Entropy **14**, 1717 (2012). arXiv:1207.2663 [gr-qc]
21. K. Bamba, S. Nojiri, S. D. Odintsov, Modified gravity: walk through accelerating cosmology, (2013). arXiv:1302.4831 [gr-qc]
22. K. Koyama, Cosmological tests of modified gravity. Rept. Prog. Phys. **79**, 046902 (2016). arXiv:1504.04623 [astro-ph.CO]
23. Z. Yousaf, M. Sharif, M. Ilyas, M. Z. Bhatti1, Influence of $f(R)$ models on the existence of anisotropic self-gravitating systems, Eur. Phys. J. C. **77**, 691, (2017)
24. Z. Yousaf, K. Bamba, M.Z. Bhatti, Role of tilted congruence and $f(R)$ gravity on regular compact objects. Phys. Rev. D. **95**, 024024 (2017). arXiv:1701.03067 [gr-qc]
25. G.G.L. Nashed, S. Capozziell, Anisotropic compact stars in $f(R)$ gravity. Eur. Phys. J. C **81**, 481 (2021). arXiv:2105.11975 [gr-qc]

26. G.G.L. Nashed, S. Capozziell, Constraining $f(R)$ gravity by Pulsar SAX J1748.9-2021 observations, Eur. Phys. J. C. **84**, 521, (2024). arXiv:2405.09590 [gr-qc]
27. M. Malaver, Regular model for a quark star with van der Waals modified equation of state. World appl. program. **3**, 309 (2013)
28. G.M. Kontogeorgis, R. Privat, J. Jaubert, Taking another look at the van der Waals equation of state-almost 150 years later. J. Chem. Eng. Data **64**, 4619 (2019)
29. S. Kong, H. Abdusattar, Y. Yin, Y. Hu, The van der Waals-like phase transition in the FRW universe, (2022). arXiv:2108.09411 [gr-qc]
30. A. Errehymy, G. Mustafa, Y. Khedif, M. Daoud, H.I. Alrebdi, A. Abdel-Aty, Self-gravitating anisotropic model in general relativity under modified Van der Waals equation of state: a stable configuration. Eur. Phys. J. C **82**, 455 (2022)
31. A. Ditta, X. Tiecheng, A. Errehymy, G. Mustafa, S.K. Maurya, Anisotropic charged stellar models with modified van der Waals EoS in $f(Q)$ gravity. Eur. Phys. J. C **83**, 254 (2023)
32. S. Chandrasekhar, The dynamical instability of gaseous masses approaching the Schwarzschild limit in general relativity. Astrophys. J. **140**, 417 (1964)
33. L. Herrera, G. Ruggeri, L. Witten, Adiabatic contraction of anisotropic spheres in general relativity. Astrophys. J. **234**, 1094 (1979)
34. J. Cooperstein, Neutron stars and the equation of state. Phys. Rev. C **37**, 786 (1988)
35. R. Chan, L. Herrera, N.O. Santos, Dynamical instability in the collapse of anisotropic matter. Class. Quantum Gravity **9**, L133 (1992)
36. Ch.C. Moustakidis, The stability of relativistic stars and the role of the adiabatic index. Gen. Rel. Grav. **49**, 68 (2017)
37. S.E. Perez Bergliaffa, Constraining $f(R)$ theories with the energy conditions. Phys. Lett. B **642**, 311 (2006)
38. J. Santos, M.J. Reboucas, J.S. Alcaniz, Energy conditions constraints on a class of $f(R)$-gravity. Int. J. Mod. Phys. D. **19**, 1315 (2010). arXiv:0807.2443 [astro-ph]
39. J. Wang, K. Liao, Energy conditions in $f(R, Lm)$ gravity, Class Quantum Grav. **29**, 215016, (2012). arXiv:1212.4656 [physics.gen-ph]
40. M. Shiravand, Z. Haghani, S. Shahidi, Energy conditions in mimetic-$f(R)$ gravity, (2017). arXiv:1507.07726 [gr-qc]
41. K. Bamba, M. Ilyas, M.Z. Bhatti, Z. Yousaf, Energy conditions in modified $f(G)$ gravity. Gen. Rel. Grav. **49**, 112 (2017). arXiv:1707.07386 [gr-qc]
42. S.A. Mardana, I. Noureenb, A. Khalid, Charged anisotropic compact star core-envelope model withpolytropic core and linear envelope. Eur. Phys. J. C **81**, 912 (2021)
43. A. Ashtekar, New Hamiltonian formulation of general relativity. Phys. Rev. D. **36**, 1587 (1987)
44. H.P. Pfeiffer, J.W. York, Extrinsic curvature and the Einstein constraints. Phys. Rev. D. **67**, 044022 (2003). arXiv:gr-qc/0207095
45. Z. Yousaf, Stellar filaments with Minkowskian core in the Einstein-Λ gravity. Eur. Phys. J. Plus. **132**, 276 (2017)
46. A.V. Astashenok, S. Capozziello, S.D. Odintsov, V.K. Oikonomou, Causal limit of neutron star maximum mass in f(R) gravity in view of GW190814. Phys. Lett. B **816**, 136222 (2021)
47. A.V. Astashenok, S. Capozziello, S.D. Odintsov, V.K. Oikonomou, Maximum baryon masses for static neutron stars in f(R) gravity. EPL **136**, 59001 (2021). arXiv:2111.14179 [gr-qc]
48. B.K. Harrison, K.S. Thorne, M. Wakano, J.A. Wheeler, Gravitational theory and gravitational collapse. Univer. Chicago Press. **194**, 177 (1965)